

Percolative conduction in anisotropic media: A renormalization-group approach

C. J. Lobb, D. J. Frank, and M. Tinkham

Division of Applied Sciences and Department of Physics, Harvard University, Cambridge, Massachusetts 02138

(Received 11 August 1980)

We apply renormalization-group transformations to a square random resistor lattice with conductance anisotropy. The bulk conductance of the lattice is studied as the bond probability and degree of anisotropy are varied. The transformations yield qualitatively correct results, although differences from numerical simulations increase as the degree of anisotropy is increased. The bulk conductance of the lattice becomes isotropic near the percolation threshold but only in an asymptotic region which shrinks as the lattice becomes more anisotropic. Near the percolation threshold the anisotropy in the macroscopic conductance vanishes as $(p - p_c)^\lambda$, where $\lambda = 0.86 \pm 0.1$.

I. INTRODUCTION

The transport properties of randomly inhomogeneous anisotropic materials have been the subject of a number of recent studies. These materials are a random mixture of two components with different (isotropic) transport properties, where the anisotropy results from characteristic dimensions of the single-component regions being different in different directions. Anisotropic superconducting-normal metal mixtures,¹ metal-insulator systems,² and metal-metal composites³ all have interesting properties from both theoretical and practical viewpoints.

The anisotropic continuum problem has received some theoretical treatment, mostly through the effective medium theory (EMT).^{4,5} To consider critical behavior, however, a lattice model is desirable as it allows the use of fairly simple renormalization-group (RG) techniques.⁶⁻¹⁰

In this paper we consider a two-dimensional random resistor lattice in which the conductance distribution rather than the geometrical correlation function is anisotropic. This is an appropriate problem because the continuum analog of this lattice model can be transformed into a geometrically anisotropic system with isotropic conductivities.² This problem has been studied using a critical-path analysis,¹¹ the EMT,¹² and analog and digital simulation.^{2,12-15} We will emphasize the renormalization-group approach here.

In Sec. II, the renormalization transformation is defined and results are obtained outside the critical region. These results are compared to the EMT and to our numerical simulations. In Sec. III, we concentrate on the region near p_c , calculating the bulk conductivity and estimating the extent of the asymptotic region. The critical exponent λ of the anisotropy is

estimated by a number of methods in Sec. IV. We compare our results to earlier experiments and simulations in Sec. V.

II. PROPERTIES NEAR $p = 1$

Consider an infinite square lattice of lattice spacing l , where the conductances g_x and g_y between nearest-neighbor sites are chosen at random, such that

$$g_x = \begin{cases} 1 & \text{with probability } p \\ 0 & \text{with probability } 1-p \end{cases}, \quad (1)$$

$$g_y = \begin{cases} \alpha & \text{with probability } p \\ 0 & \text{with probability } 1-p \end{cases}. \quad (2)$$

The microscopic anisotropy ratio α ranges between 0 and ∞ . The bond probability p is taken to be the same in both directions so that the percolation threshold and coherence length are independent of the conductance anisotropy ratio.¹⁶

Following the scheme discussed by Bernasconi, we rescale by partitioning the lattice into cells of size bl and replacing each cell by a single conductance in each direction.⁸ The rescaled conductance in a given direction is defined to be equal to the conductance of an isolated cell with parallel equipotentials imposed on the appropriate sides (see Fig. 1). We have chosen this rescaling rule for a number of reasons. When $p = 1$, this rule predicts the rescaled anisotropy correctly. By contrast, schemes which calculate a rescaled conductance between two points are incorrect for anisotropic lattices, as will be shown in Sec. III. In addition, equipotential boundaries make the infinite b limit of this rule equivalent to the original prob-

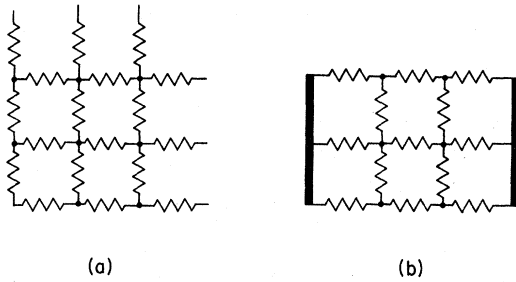


FIG. 1. (a) Cell used for the $b = 3$ RG transformation. Equipotentials are imposed on the left and right, effectively reducing the cell to that shown in (b), to calculate the rescaled conductance in the x direction.

lem, which is to calculate the conductance per square of the infinite lattice. The increasing accuracy of our method as b is increased allows us to judge its reliability for small b by going to the more difficult large b limit, as we do in Sec. IV. Finally, the particular equipotential boundary cells used here, being self-dual, incorporate an important symmetry property of the lattice.⁸ This guarantees that any properties which result from the self-dual symmetry (such as the value of the percolation threshold $p_c = \frac{1}{2}$) will necessarily be given correctly when cells of this type are used.⁸

In principle, the transformation is repeatedly applied to the lattice, giving a sequence of conductance distributions which eventually converges to a single δ function for each direction (provided $p \neq p_c$ initially). These δ functions are centered at conductances $\hat{G}_x(b)$ and $\hat{G}_y(b)$. These conductances are only approximations to the lattice conductivity in the two directions because b is finite. In practice, we use approximations to $\hat{G}_x(b)$ and $\hat{G}_y(b)$ which replace each intermediate distribution of conductances by simple double-valued distributions. All of the nonzero conductances in each distribution are replaced by a single conductance which is the geometric mean of the nonzero conductances.⁸ This process eventually converges to conductances which are labeled $\hat{G}_{x, \text{approx}}(b)$ and $\hat{G}_{y, \text{approx}}(b)$. We calculate $\hat{G}_{x, \text{approx}}(b)$ and $\hat{G}_{y, \text{approx}}(b)$ for $b = 3$ by going through all of the possible configurations on a computer. Monte Carlo methods are employed for $b = 3$ to calculate $\hat{G}_x(b)$ and $\hat{G}_y(b)$.

Data for a number of anisotropies are presented in Figs. 2–4 using $\hat{G}_{x, \text{approx}}(b)$ for the $b = 3$ transformation. [We compared $\hat{G}_{\text{approx}}(b)$ to $\hat{G}(b)$ for a number of these points and concluded that they are essentially equal for the range of anisotropies considered here.] The RG data are plotted with the EMT prediction and the results of Monte Carlo simulations on random 50-by-50 site arrays of resistors. These arrays had equipotentials imposed on the left

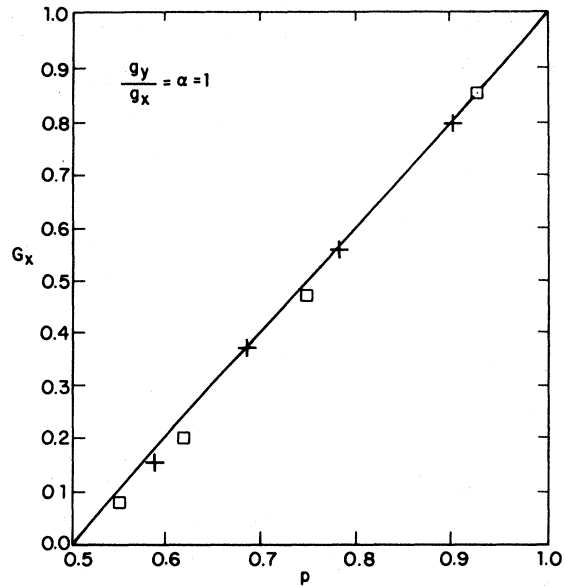


FIG. 2. Conductance vs concentration for $\alpha = 1$ from the EMT (solid curve), numerical simulations (+), and the $b = 3$ RG (\square).

and right, and periodic boundary conditions on the top and bottom. Overrelaxation of Kirchoff's law was used.¹⁷ Lattices were solved by removing a few resistors, relaxing the voltages, and repeating the process until the desired value of p was reached. Close to the percolation threshold, the "insulating" ele-

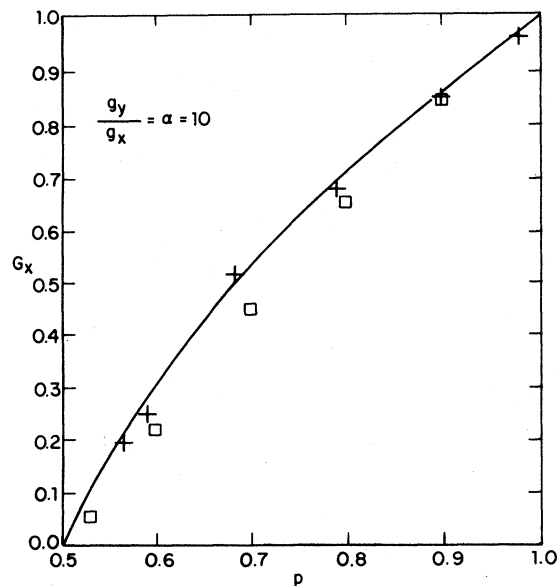


FIG. 3. Conductance vs concentration for $\alpha = 10$ from the EMT (solid curve), numerical simulations (+), and the $b = 3$ RG (\square).

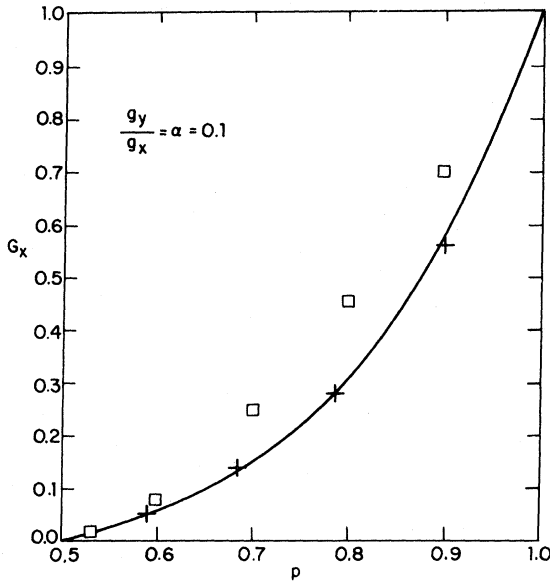


FIG. 4. Conductance vs concentration for $\alpha=0.1$ from the EMT (solid curve), numerical simulations (+), and the $b=3$ RG (o).

ments were started out with a conductivity equal to that of the conducting elements. The network was solved by gradually decreasing the conductance of the "insulating" elements. Convergence was slow near the percolation threshold, even using a fairly large computer, a DEC PDP-10.

For the isotropic ($\alpha=1$) case Bernasconi has shown⁸ that the EMT, numerical simulations and the renormalization transformations give essentially the same results near $p=1$. In the region near p_c where the EMT breaks down, the $b=2$ transformation has been studied and agrees well with numerical simulations.⁸ Our data for $b=3$ (Fig. 2) agree well with these results.

For $\alpha=10$ (Fig. 3), the EMT and numerical simulations agree well for p near 1. (Convergence problems and finite-size effects make comparison difficult for p near p_c .) However, the $b=3$ RG transformation *underestimates* the bulk conductance in this case.

When $\alpha=0.1$ (Fig. 4), the EMT and numerical simulations again agree outside the critical region. The disagreement with the RG, however, is quite pronounced. For this case, the RG *overestimates* the bulk conductance.

These discrepancies are easy to understand. For the $b=3$ transformation, only 4 of the 13 conductors in an x -direction cell have value α , as compared to one-half of the conductors in the lattice itself (see Fig. 1). Thus, any effects due to $\alpha \neq 1$ will be underestimated for a finite-size cell transformation. For $\alpha=0.1$, $p=0.9$, we obtain $G_x=0.576$ from the EMT and $G_x \approx 0.56$ from numerical simulations, while the

$b=2$ RG predicts $\hat{G}_x(b)=0.73$ and the $b=3$ RG predicts $\hat{G}_x(b)=0.69$. Thus, the larger cell, which has a higher fraction of conductors pointing in the y direction, gives an answer closer to the truth, although neither cell is very accurate. Since the fraction of conductors pointing in the y direction is given to first order by $(1-1/b)/2$, it is reasonable to plot $\hat{G}_x(b)$ against $1/b$ and extrapolate to $b=\infty$. The $b=2$ and 3 points extrapolate to 0.61, in fair agreement with the numerical and EMT values, especially considering the limited data on which to base the extrapolation.

It is tempting to try to find cells which deal with anisotropy more accurately. One could use cells in which the top row of conductors is not cut off, but this only increases the number of vertical conductors to 6 out of 18 (from 4 out of 13) for a $b=3$ cell. This also sacrifices the self-dual symmetry of the cells, so that the wrong value of p_c is predicted. Other procedures, such as weighting the vertical conductors more heavily in the average, could probably be made to work, but suffer from being arbitrary.

III. IN ASYMPTOTIA

In spite of the inaccuracies described above, the RG is a useful tool for studying the critical region. The method gives answers which are at least qualitatively reasonable, if not quantitatively correct, and it is quite simple computationally. This last advantage is critical close to the percolation threshold where the EMT breaks down and numerical methods encounter serious difficulties as convergence slows down and sample-to-sample variations become large. Thus, the RG is the only choice presently available *arbitrarily* close to the percolation threshold. Hopefully, information obtained by it will be at least qualitatively correct.

The conductance of isotropic square lattices varies as $(p-p_c)^t$ where $t \approx 1.35$ for $p-p_c$ small.^{9,10,18} For $0 < \alpha < \infty$, it has been rigorously shown^{2,19} that, in the limit as p approaches p_c , the same critical exponent t characterizes systems which differ only in their anisotropy ratio α . This is true because the bulk conductance as a function of p is bounded above and below by the conductance of isotropic lattices where the nonzero conductances are either all 1 or all α (see Fig. 5). There is also evidence based on a critical path analysis¹¹ for the stronger conjecture that the bulk lattice conductance becomes isotropic as p approaches p_c . The renormalization group agrees with both of these results, predicting that the bulk anisotropy ratio $A = \hat{G}_{y, \text{approx}}(b) / \hat{G}_{x, \text{approx}}(b)$ approaches 1 as p approaches p_c . This is true because the sequence $\alpha^{(1)}, \alpha^{(2)}, \dots, \alpha^{(n)}$ of anisotropy ratios of the intermediate rescaled distributions approaches 1 for α not equal to zero at $p=p_c = \frac{1}{2}$.

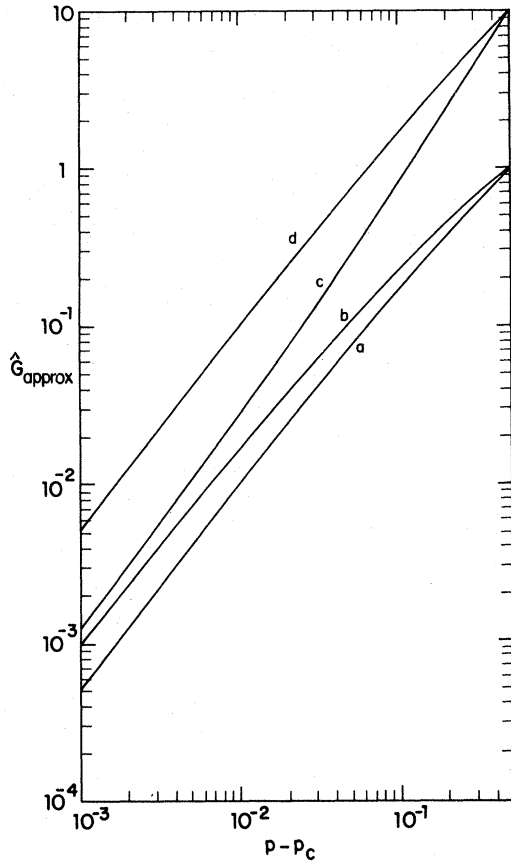


FIG. 5. Conductance in the x direction vs concentration as calculated by the $b = 3$ RG. $(g_x, g_y) = (1, 1), (1, 10), (10, 1), (10, 10)$ for curves a–d.

There are, however, significant differences between anisotropic and isotropic lattices, even near p_c . Figure 6 shows an effective critical exponent $\hat{t}(p)$, defined as $\partial \log \hat{G}_{x, \text{approx}}(b) / \partial \log(p - p_c)_s$, for various values of α , obtained from the $b = 3$ transformation. As p approaches p_c , $\hat{t}(p)$ approaches t , because G varies as $(p - p_c)^t$ arbitrarily close to p_c . The quantity $\hat{t}(p)$ converges to t much faster as p approaches p_c for the isotropic lattice than for highly anisotropic ones. Thus, if we operationally define the critical region as the range of p over which $\hat{t}(p)$ is within a given percentage of t , the critical region shrinks as a result of anisotropy. Experimentally, this means that one needs to be closer to p_c to extract a good value of t from data on a highly anisotropic system than from data on an isotropic system.

The quantity $\hat{t}(p)$ was first studied for isotropic lattices for the $b = 2$ transformation.⁸ Our data for $b = 3$ for the isotropic case agrees well with the earlier $b = 2$ results, supporting Bernasconi's conjecture that numerical (non-RG) estimates of t are too low since they must use data which typically extend to

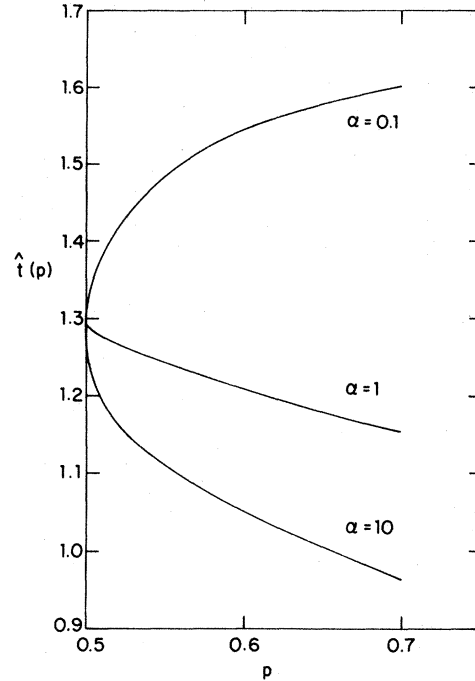


FIG. 6. Effective exponent $\hat{t}(p)$ vs p for various anisotropies α , as calculated from the $b = 3$ RG.

$p - p_c = 0.1$. Calculation of $\hat{t}(p)$ for larger values of b could clear up the discrepancies between the best numerical estimate²⁰ $t = 1.1 \pm 0.05$ and the large-cell ($b = 14$) RG estimate^{9,10} $t = 1.35 \pm 0.02$.

We can use Fig. 5 to obtain a bound on the uncertainty in t . Since the true conductance is rigorously bounded above and below by the isotropic results approximated by curves a and d, its logarithmic derivative $\hat{t}(p)$ can deviate from t by no more than roughly $\log(\alpha^{1/2}) / \log(p - p_c)$. In fact, the data in Fig. 6 (which are based on the $b = 3$ RG) are well approximated by

$$\hat{t}(p) = 1.29 + 0.4 \log(\alpha^{1/2}) / \log(p - p_c) \quad (3)$$

for $\alpha = 0.1$ and 10. For $\hat{t}(p)$ to be within 0.01 of t , this says that $(p - p_c) < \alpha^{\pm 20}$ (+ for $\alpha < 1$, - for $\alpha > 1$), which is a very stringent requirement. For example, it requires $(p - p_c) < 10^{-6}$ if α differs from unity by only a factor of 2.

A number of different lattice renormalization schemes have been used. Most of them differ from the one used here in that they calculate the conductance between two points in a lattice⁷ (see Fig. 7). Cells with equipotential boundaries, such as we use here, correctly predict that $A = \alpha$ at $p = 1$. In contrast, the cell in Fig. 7 predicts $\alpha' = \alpha(\alpha + 3) / (3\alpha + 1)$ after one iteration at $p = 1$, which incorrectly implies that $A = \alpha$ only for $\alpha = 0, 1$, or ∞ when $p = 1$.

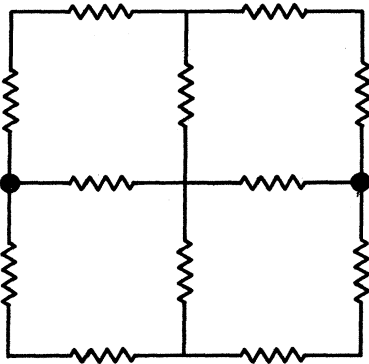


FIG. 7. Alternative cell for RG calculations. The rescaled conductance is calculated between two points instead of between two equipotential lines.

IV. CRITICAL EXPONENT λ

Near the percolation threshold, it is plausible to assume that $A(p, \alpha) - 1 \propto (p - p_c)^\lambda$ since the macroscopic anisotropy ratio approaches one as $p - p_c$ approaches zero.¹¹ When $\log[A(p, \alpha) - 1]$, as derived from the data of Fig. 5, is plotted against $\log(p - p_c)$, we find that $\lambda \geq 0.34$ (the slope increases slowly as p approaches p_c).

The exponent λ may also be calculated using a renormalization-group approach directly. Using $\log A$ and $\log \alpha$ as variables, we assume that

$$\log A(p, \alpha) \propto (\log \alpha)(p - p_c)^\lambda. \quad (4)$$

We have chosen this form because it satisfies the requirement that $A(p, 1/\alpha) = 1/A(p, \alpha)$. It also reflects the fact that $A(p, \alpha = 1) = 1$ independently of p . (We note that the variable $\alpha - 1$ could have been used because $\ln \alpha \approx \alpha - 1$ for α near 1.) Upon renormalizing we infer that

$$(\log \alpha')(p' - p_c)^\lambda = (\log \alpha)(p - p_c)^\lambda, \quad (5)$$

where p' is the rescaled bond probability and α' is the rescaled conductance anisotropy ratio. Thus

$$\lambda = \lim_{\substack{\alpha \rightarrow 1 \\ p \rightarrow p_c}} \log \left(\frac{\log \alpha}{\log \alpha'} \right) / \log \left(\frac{\partial p'}{\partial p} \right), \quad (6)$$

where the limit is taken to ensure that we are at the critical point. For $b = 2$, the quantities in (6) can be calculated exactly. Using the geometric mean of the conductance in each direction to define α' we find that $\lambda = 0.254$ for $b = 2$. For $b = 3$, a program which generated all of the possible configurations was used to calculate the rescaled conductances. This gave $\lambda = 0.371$ for $b = 3$.

Larger cells are expected to give more accurate es-

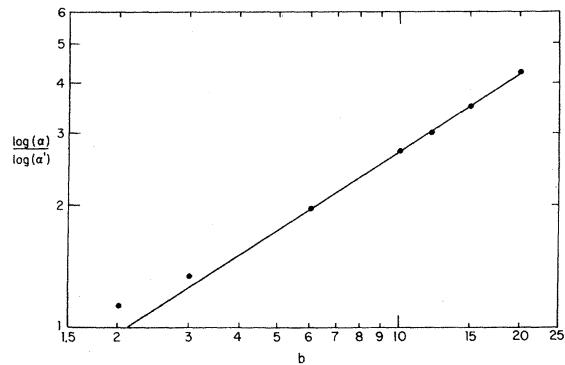


FIG. 8. Log-log plot of $\log \alpha / \log \alpha'$ against b . The slope of this line is λ/ν in the limit of large b .

timates of critical parameters. Arguments concerning the errors introduced by small cells for calculating other critical exponents suggest that a more accurate version of (6) is^{21,22}

$$\log \left(\frac{\log \alpha}{\log \alpha'} \right) \sim \frac{\lambda}{\nu} \log b + \text{const}, \quad (7)$$

where b is the cell size and $\nu = \log b / \log(\partial p' / \partial p)|_{p_c}$ is the correlation length exponent ≈ 1.34 in two dimensions.²¹⁻²³ Thus, a log-log plot of $\log \alpha / \log \alpha'$ vs b should approach a straight line for large b , the slope of which equals λ/ν .

We calculated α' analytically for $b = 2$ and numerically for $b = 3$ using a program which enumerated all of the possible configurations. For b larger than 3, we used a program which calculated the conductance of each Monte Carlo realization of a cell exactly.^{9,10}

Figure 8 contains the data thus obtained using $\alpha = 1.1$. We note that smaller α 's gave essentially the same value for $\log \alpha / \log \alpha'$. The slope of the line fitted from $b = 6$ through 20 is 0.64 ± 0.07 , where the error is an estimate of the effects of including or not including the smaller cell data in the fit. Using $\nu = 1.343 \pm 0.017$,²³ we conclude that $\lambda = 0.86 \pm 0.1$. This estimate is larger than that obtained from (6) because the constant in (7) is not small, as can be seen from Fig. 8.

V. COMPARISON WITH EARLIER WORK

A system to which our model calculations apply has recently been reported.² The conductivities of percolative networks produced photolithographically from laser speckle patterns were measured. These results are shown in Fig. 9 for various aspect ratios of metal islands. The results of numerical simulations on a 50-by-50 site lattice for the corresponding α 's are shown in the inset. The qualitative agreement is striking, demonstrating that a simple lattice model is

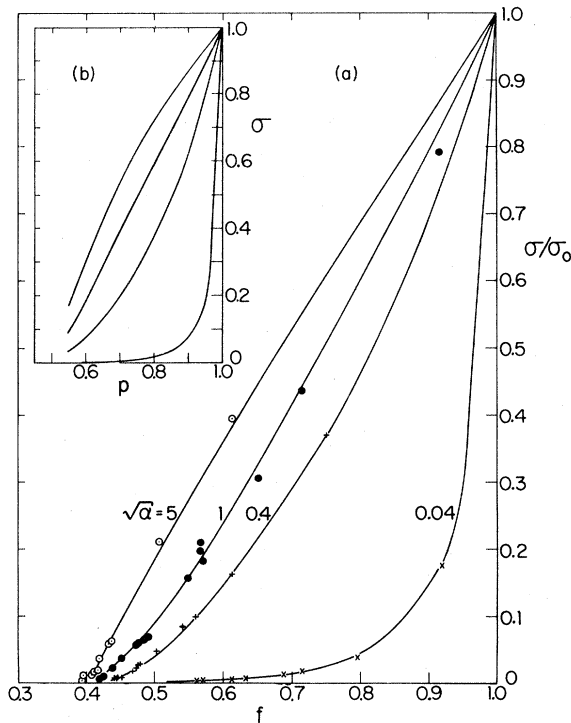


FIG. 9. Normalized conductance vs area fraction for anisotropic metal islands on an insulating substrate. The solid lines are to guide the eye. Inset contains numerical simulations on 50×50 site lattices with the corresponding anisotropies. The aspect ratio of the islands L_x/L_y is equal to $\alpha^{1/2}$, as can be seen from Refs. 11 and 2. We note that the islands have a critical area fraction of about 0.4 while the lattices have a p_c of 0.5.

quite good. The experimental data are consistent with Fig. 6, in that the measured exponent depends on anisotropy if the critical region is assumed to be the same for all anisotropies. When the speckle pattern data was fit to 15% above the percolation threshold, effective exponents $\hat{t} = 0.85, 1.75,$ and 2.3 were obtained for $\alpha = 25, 0.16,$ and 0.0016 . Using $t = 1.3$ and $\hat{t}(f) = t + 0.4 \log(\alpha^{1/2})/\log(f - f_c)$ as suggested by the lattice model gives $\hat{t}(f) = 0.95, 1.48,$ and 1.97 . The agreement is quite good considering the approximations made. We note that the effects of anisotropy are again underestimated by the small cell used.

Sarychev and Vinogradoff have reported numerical simulations on 50-by-50 site lattices.¹⁴ They concluded that the conductance varied as $(p - p_c)^t$ with $t \approx 1.25$ for a range of concentrations extending 0.1 or more above p_c , independently of α . This is in contrast with this work and earlier results² which found that the fitted exponent varied with the anisotropy if the fit extended to 0.15 above p_c . We note

that α ranged between 0.3 and 3.33 in the simulations of Sarychev and Vinogradoff. Equation (3) predicts a variation in \hat{t} of only 8% from t for this range of anisotropy, an amount which could be masked by their quoted uncertainties of $\pm 12\%$.

Sarychev and Vinogradoff also report that the bulk anisotropy ratio A does not approach unity as p approaches p_c , that is, that λ is 0. This disagrees with our result that $\lambda = 0.86$. Their data are not inconsistent with our picture, however. Figure 5 shows that A approaches 1 quite slowly near p_c , still being of order 1.5 for $\alpha = 10$ at $p = 0.501$ (the smallest p that we studied). This slow approach of A to 1 is important since Monte Carlo data are limited by the requirement that the coherence length ξ be much smaller than the sample size for the sample to be effectively infinite. Using $\xi \approx |2(p - p_c)|^{-\nu}$, this suggests the constraint

$$|p - p_c| \gg (1/2)L^{-1/\nu} \quad (8)$$

For $L = 50$, as in their work, this becomes $|p - p_c| \gg 0.03$, so that data for p lower than 0.53 must not be accepted as representative of infinite sample data.

Mendelson and Karioris¹⁵ report analog simulations (punched holes in conducting paper) on a number of different samples and find that the bulk anisotropy ratio A varies greatly from sample to sample as p approaches p_c . These fluctuations are due to the finite sizes of the samples studied, and probably account for the results of Sarychev and Vinogradoff.

Blanc, Mitescu, and Thevenot¹³ have studied a different anisotropic conductance problem. Their lattices consisted of resistors with the same resistance in each direction, but with the bond probability being anisotropic. They found that their fitted exponent \hat{t} varied with the anisotropy in much the same way as ours does, and also concluded (as do we) that the asymptotic region becomes smaller as the lattice becomes more anisotropic.

VI. CONCLUSIONS

We have studied the effects of conductance anisotropy on the bulk properties of square random resistor lattices using a renormalization-group approach. Near $p = 0.5$ and 1, this approach predicts reasonable values for the bulk anisotropy and conductance. In the range between, predictions which are qualitatively correct result, although quantitative agreement is poor due to small-cell-size effects.

The extent of the asymptotic region depends on the degree of anisotropy. In general, as α differs further from 1, the asymptotic region shrinks. As p approaches p_c , we find that the lattice becomes isotro-

pic, that is, that A approaches 1. The exponent λ which characterizes the bulk anisotropy near p_c was found to be 0.86 ± 0.1 .

A number of related problems can be studied by similar techniques. Consideration of the problem of combined conductance and bond probability anisotropy should lead to interesting results. The anisotropic three-dimensional problem is also interesting, as it should allow one to study the crossover to two dimensions, a case which is less trivial than the cross-

over from two dimensions to one dimension which is our $\alpha = 0$ limit.

ACKNOWLEDGMENTS

We are grateful to David R. Nelson, L. N. Smith, and W. J. Skocpol for useful discussions in the course of this work. This research was partially supported by the NSF.

-
- ¹C. J. Lobb, M. Tinkham, and W. J. Skocpol, *Solid State Commun.* **27**, 1273 (1978).
- ²L. N. Smith and C. J. Lobb, *Phys. Rev. B* **20**, 3653 (1979).
- ³Keith R. Karasek and J. Bevk, *Scr. Metall.* **13**, 259 (1979).
- ⁴D. Stroud, *Phys. Rev. B* **12**, 3368 (1975).
- ⁵A. Davidson and M. Tinkham, *Phys. Rev. B* **13**, 3261 (1976).
- ⁶A. P. Young and R. B. Stinchcombe, *J. Phys. C* **8**, L535 (1975).
- ⁷R. B. Stinchcombe and B. P. Watson, *J. Phys. C* **9**, 3221 (1976).
- ⁸J. Bernasconi, *Phys. Rev. B* **18**, 2185 (1978).
- ⁹C. J. Lobb and D. J. Frank, *J. Phys. C* **12**, L827 (1979).
- ¹⁰C. J. Lobb and D. J. Frank, in *Inhomogeneous Superconductors*, edited by D. U. Gubser, T. L. Francavilla, J. R. Leibowitz, and S. A. Wolf, AIP Conf. Proc. No. 58 (AIP, New York, 1980), p. 308.
- ¹¹B. I. Shklovskii, *Phys. Status Solidi (b)* **85**, K111 (1978).
- ¹²J. Bernasconi, *Phys. Rev. B* **9**, 4575 (1974).
- ¹³R. Blanc, C. D. Mitescu, and G. Thevenot, *J. Phys. (Paris)* **41**, 387 (1980).
- ¹⁴A. K. Sarychev and A. P. Vinogradoff, *J. Phys. C* **12**, L681 (1979).
- ¹⁵Kenneth S. Mendelson and Frank G. Karioris, *J. Phys. C* **13**, 6197 (1980).
- ¹⁶S. Redner and H. E. Stanley, *J. Phys. A* **12**, 1267 (1979).
- ¹⁷Itzhak Webman, Joshua Jortner, and Morrel H. Cohen, *Phys. Rev. B* **11**, 2885 (1975).
- ¹⁸S. Kirkpatrick, *Rev. Mod. Phys.* **45**, 574 (1973).
- ¹⁹B. I. Halperin (private communication).
- ²⁰S. Kirkpatrick, in *Proceedings of the Summer School on III Condensed Matter*, edited by Roger Balian, Roger Maynard, and Gerard Toulouse (North-Holland, Amsterdam, 1979).
- ²¹Peter J. Reynolds, H. Eugene Stanley, and W. Klein, *J. Phys. A* **11**, L199 (1978).
- ²²Peter J. Reynolds, H. Eugene Stanley, and W. Klein, *Phys. Rev. B* **21**, 1223 (1980).
- ²³C. J. Lobb and Keith R. Karasek, *J. Phys. C* **13**, L245 (1980).